Take-Off Engine Particle Emission Indices for In-Service Aircraft at Los Angeles International Airport

Richard H. Moore, Michael A. Shook, Luke D. Ziemba, Joshua P. DiGangi, Edward L. Winstead, Bastian Rauch, Tina Jurkat, Kenneth L. Thornhill, Ewan C. Crosbie, Claire Robinson, Taylor J. Shingler, and Bruce E. Anderson

NASA Langley Research Center, Hampton, Virginia, USA

richard.h.moore@nasa.gov

Background and Motivation

- Aircraft engine particle emissions are important contributors to local air quality near airports.
- Emissions occur during multiple stages of aircraft movement including idling at terminal gates, taxiing, runway take-offs, and runway landings, which are collectively known as the landing-takeoff cycle (LTO).
- Limited information on engine LTO particle emissions are available from manufacturers prior to certification and operation (typically reported as a smoke number).
- The LTO certification process is idealized as engine conditions are measured under discrete, steady thrust settings that may differ from thrusts actually applied by pilots.
- Consequently, there is a need to understand the emissions from these currently in-service engines under real-world conditions. Here, we investigate particle emissions emitted by aircraft during takeoff operations at Los Angeles International Airport (LAX).

Experimental

Data were collected at 400-m distance downwind of the northern take-off runway (24L) of Los Angeles International Airport (33.9509°N, 118.398°W) on two days: 18 May and 25 May 2014. Runway 24L has a declared distance of 3135 m in length, 263° true bearing, and is at an elevation of 38 m. An onshore sea breeze of 0-10 m s^{-1} and oriented down the runway (±20°) was predominant during both measurement days, which advected the aircraft take-off plumes to the sampling inlet of the NASA Langley Aerosol Research Group (LARGE) Mobile Laboratory. The height of the inlet was approximately 2 m above the ground.

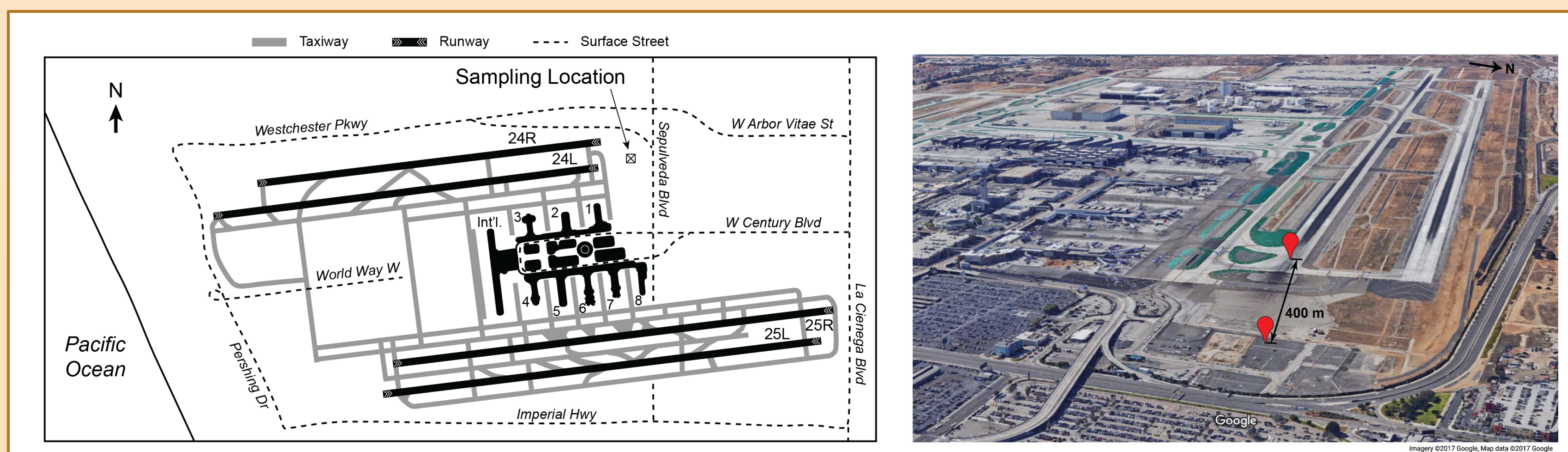

Figure 1. Schematic of Los Angeles International Airport and surrounding major surface streets (left). The sampling location is indicated by the [X] icon in the employee parking lot just west of Sepulveda Boulevard and downwind of take-off runway 24L. Aerial image of the northern portion of Los Angeles International Airport (right). Red markers denote the sampling location and the beginning of Runway 24L. The distance between the two points is about 400 m.

LAX aircraft were fueled from Tank 6014 on 18 May and from Tanks 402 and 609 on 25 May. Average fuel properties for the contents of these tanks are shown in Table 1, based on laboratory analyses of delivered fuel batches.

Table 1. Average fuel properties during the sampling period.

Fuel Property	18 May 2014	25 May 2014
Sulfur (ppmm)	1400 ± 180	1180 ± 600
Aromatics (volume %)	18.1 ± 0.6	18.8 ± 5.2
Naphthalenes (volume %)	1.06 ± 0.35	1.57 ± 1.11
Heat of Combustion (MJ kg^{-1})	43.251 ± 0.002	43.13 ± 0.14

The average fuel sulfur and aromatic contents are typical of Jet A fuel in the United States; however, the large standard deviations shown for 25 May result from particularly low sulfur and aromatic domestic fuels (600-700 ppmm and 12-18%, respectively) being mixed with fuels with higher sulfur and aromatic content from abroad (1600-1800 ppmm and 22-23%, respectively). Since fuel is issued for the entire airport on a given day, it is not possible to determine the exact composition of the fuel used to service the sampled aircraft.

Timeseries of ambient concentrations of carbon dioxide and aerosol species were measured continuously during each sampling day with discernable increases in all species associated with aircraft take-off events (Fig. 2).

Aircraft tail numbers were recorded for each take-off, which were then used to identify the aircraft and engine specifications from FAA and ICAO databases.

The emission index (EI) of particle species X is determined following Moore et al., 2017, as

$$EI_X = \frac{\Delta X}{\Delta CO_2}\frac{V_m}{M_{CO_2}}\left(EI_{CO_2}\right)$$

$$\text{where, } EI_{CO_2} = \frac{RT}{PV_m}\frac{M_{CO_2}}{\left(M_C + \alpha M_H\right)} \sim 3160 \text{ gCO}_2 \text{ kg-fuel}^{-1},$$

ΔX and ΔCO_2 are the background-subtracted peak areas of the measured concentrations of species X and CO_2 at STP, respectively; EI_{CO2} is the emissions index of CO_2, assuming that the carbon content in the fuel is constant and is completely converted to CO_2; R is the ideal gas constant; T is the temperature at STP (273.15 K); P is the pressure at STP (1 atm); V_m is the molar volume of ideal gas at STP (22.4 L mol^{-1}); α is the fuel hydrogen-to-carbon molar ratio (assumed to be 1.92); and M_{CO2}, M_C, M_H are the molar masses of CO_2, carbon, and hydrogen, respectively.

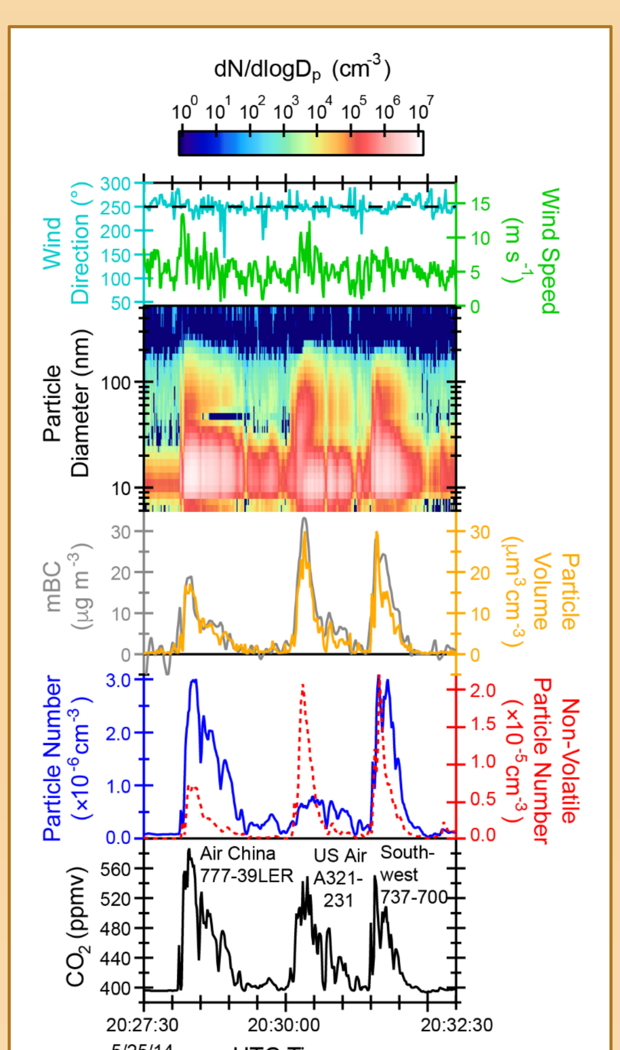

Figure 2. Example timeseries of measured parameters showing three aircraft take-off plumes.

Results

Overall, 275 take-off plumes were sampled during the 18 May and 25 May 2014 study period. The most common aircraft plumes sampled were those from small-to-medium-size regional aircraft with CFM56 engines, GE CF34 engines, PW118, and IAE2500 engines.

Table 2. Summary of sampled aircraft engines, airframes, and emission indices (EI)

Engine manufacturer, model, and series	Aircraft manufact-urer	Years of aircraft manufact-ure	Aircraft model and series	No. of plumes sampled	Particle number EI (kg^{-1})	Non-volatile particle number EI (kg^{-1})	BC-equivalent particle mass EI (mg kg^{-1})
CFM CFM56-3B	Boeing	1987-1997	737-300, 737-500	20	3.56×10^{16} ⁎ 1.41	2.54×10^{15} ⁎ 2.35	564 ⁎ 1.41
CFM CFM56-3C	Boeing	1998	737-400	1	1.65×10^{16}	2.31×10^{15}	792
CFM CFM56-5A	Airbus	1990-1998	A319-100, A320-200	11	4.62×10^{16} ⁎ 1.25	1.85×10^{15} ⁎ 2.50	419 ⁎ 1.37
CFM CFM56-5B	Airbus	1999-2013	A319-100, A320-200, A321-200	40	5.09×10^{16} ⁎ 1.39	1.78×10^{15} ⁎ 2.20	276 ⁎ 1.51
CFM CFM56-5C	Airbus	2001	A340-300	2	5.06×10^{16} ⁎ 1.02	1.11×10^{15} ⁎ 1.55	416 ⁎ 1.08
CFM CFM56-7B	Boeing	1998-2014	737-700, 737-800, 737-900	86	5.23×10^{16} ⁎ 1.31	2.18×10^{15} ⁎ 2.35	354 ⁎ 1.51
GE CF34-3	Bombardier	2000-2003	CRJ-200	6	3.62×10^{16} ⁎ 1.50	4.99×10^{15} ⁎ 1.34	488 ⁎ 1.59
GE CF34-8	Bombardier, Embraer	2006-2011	CRJ-700, CRJ-900, ERJ-170	23	2.98×10^{16} ⁎ 1.74	2.67×10^{15} ⁎ 1.79	428 ⁎ 1.49
GE CF6-80C2	Boeing	1989-2012	747-400, 767-300	6	3.83×10^{16} ⁎ 1.45	1.06×10^{15} ⁎ 2.54	190 ⁎ 1.49
GE GE90-94B	Boeing	2002-2003	777-200	2	3.95×10^{16} ⁎ 1.16	5.12×10^{14} ⁎ 1.13	92.8 ⁎ 1.12
GE GE90-115B	Boeing	2003-2012	777-300, 777-300	6	3.39×10^{16} ⁎ 1.20	7.95×10^{14} ⁎ 1.96	175 ⁎ 1.30
GE GEnx-2B67	Boeing	2012-2014	747-800	2	8.83×10^{16} ⁎ 1.41	1.95×10^{15} ⁎ 4.07	46.1 ⁎ 1.48
EA GP7270	Airbus	2010-2013	A380-800	3	2.86×10^{16} ⁎ 1.25	1.89×10^{15} ⁎ 1.18	129 ⁎ 1.33
PW JT8D	McDonnell Douglas	1987	MD-80	2	1.73×10^{16} ⁎ 2.89	2.83×10^{15} ⁎ 2.53	941 ⁎ 1.06
PW PT6A	Beech	1996	1900D	7	3.86×10^{16} ⁎ 1.89	7.09×10^{15} ⁎ 1.93	477 ⁎ 1.93
PW PW118	Embraer	1994-1999	ERJ-120	10	5.80×10^{16} ⁎ 1.33	2.98×10^{15} ⁎ 1.69	649 ⁎ 1.62
PW 150A	Bombardier	2004-2013	DHC-8	3	5.87×10^{16} ⁎ 1.26	4.49×10^{15} ⁎ 3.56	252 ⁎ 1.51
PW PW2000	Boeing	1984	757-200	1	2.46×10^{16}	2.55×10^{15}	817
PW PW4000	Airbus, Boeing	2002	A330-200, 767-300	2	8.80×10^{15} ⁎ 1.06	1.70×10^{15} ⁎ 1.22	439 ⁎ 1.65
Rolls-Royce AE3007	Embraer	1999-2007	ERJ-145	2	2.61×10^{16} ⁎ 3.11	1.45×10^{15} ⁎ 1.02	592
Rolls-Royce RB211	Boeing	1992-1993	747-400, 757-200	2	4.12×10^{16} ⁎ 1.39	1.07×10^{15} ⁎ 2.08	196 ⁎ 1.25
Rolls-Royce Trent 556	Airbus	2003-2009	A340-600	2	2.83×10^{16} ⁎ 1.28	1.06×10^{15} ⁎ 3.99	319 ⁎ 1.49
Rolls-Royce Trent 772	Airbus	2009	A330-200	2	2.49×10^{16} ⁎ 1.32	1.06×10^{15} ⁎ 1.37	177 ⁎ 1.01
Rolls-Royce Trent 892	Boeing	2006	777-200	1	3.04×10^{16}	8.09×10^{14}	304
Rolls-Royce Trent 970	Airbus	2011-2013	A380-800	3	5.13×10^{16} ⁎ 1.17	8.44×10^{14} ⁎ 1.60	356 ⁎ 1.23
IAE V2522	Airbus	1998	A319-100	1	2.58×10^{16}	2.86×10^{15}	584
IAE V2524	Airbus	2005-2007	A319-100	2	1.14×10^{16} ⁎ 1.15	3.42×10^{15} ⁎ 2.10	786 ⁎ 1.21
IAE V2527	Airbus	2000-2013	A319-100, A320-200	17	1.93×10^{16} ⁎ 1.75	2.36×10^{15} ⁎ 1.73	414 ⁎ 1.33
IAE V2533	Airbus	2008-2014	A321-200	10	2.09×10^{16} ⁎ 1.98	1.90×10^{15} ⁎ 3.15	343 ⁎ 1.29

Emissions indices reported as the geometric mean ⁎ 1 geometric standard deviation (g.s.d). Note that kg^{-1} denotes 'per kilogram of fuel'.

The relationships between measured EIs are shown in Fig. 3, where each point is a single plume. Summary statistics for selected EIs averaged by engine type are reported in Table 2.

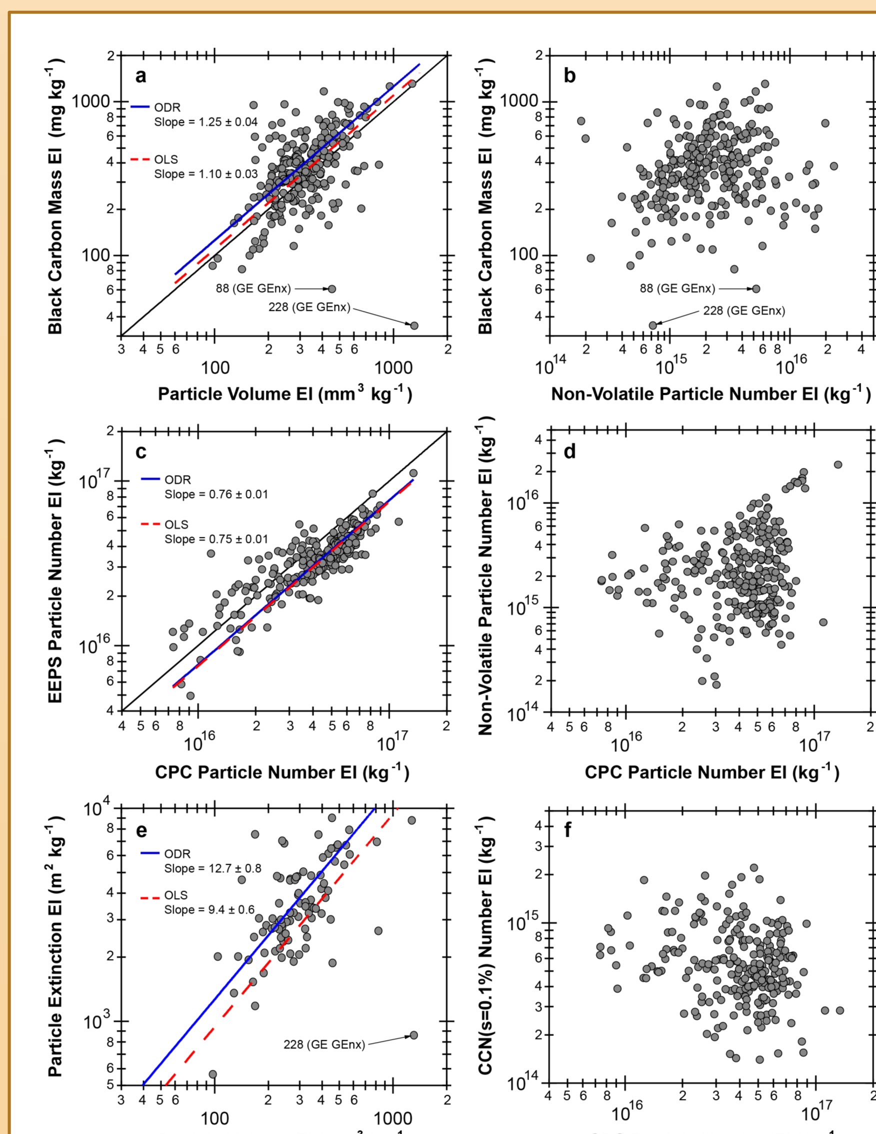

Figure 3. Scatter plots showing the relationship between measured particle emissions indices (EIs). Solid lines are orthogonal distance regression (ODR) linear fits to the data, while dashed lines are ordinary least squares (OLS) linear fits. For both fits, the intercept was held at zero. Outlier test points 88 and 228 are noted, which correspond to the two plume intercepts of the GE GEnx engine. Note that kg^{-1} denotes 'per kilogram of fuel'.

Good correlation is observed between the MAAP-derived black carbon mass EI and particle volume EI from the EEPS. Similarly, the EEPS integrated number EI shows good linearity with the CPC measurement; noting that the CPC and EEPS have different lower cutoff sizes, which explains the non-unity slope.

Average particle number and volume size distributions from the EEPS are shown in Fig. 4, which are similar in shape to the distributions observed by Lobo et al., 2012.

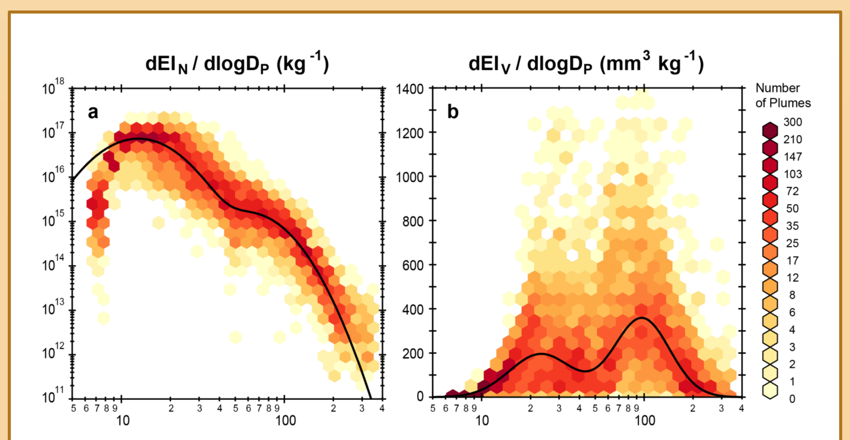

Figure 4. Size distributions of take-off particle number emissions index (a) and volume emissions index (b). Each of the 275 sampled plumes are binned as denoted by the coloured hexagons. The solid lines are two-mode, log-normal fits to the geometric mean distribution of all plumes for which size distribution data are available (N=253).

Summary & Conclusions

- Emission indices from 275 distinct aircraft takeoff plumes are reported for a variety of engine types and aircraft configurations.
- Particle number EIs are in the range of 10^{16}-10^{17} kg-fuel^{-1} on a number basis and 100-1000 mg kg-fuel^{-1} on a mass basis, which are consistent with previous advected plume measurements (e.g., Lobo et al., 2012).
- This work substantially expands the database of takeoff emissions indices both in terms of plumes sampled and diversity of engine types.

References

- Moore, R.H. et al. (2017) *Nature*, 543(7645): 411-415. doi:10.1038/nature21420
- Lobo, P. et al. (2012) *Atmospheric Environment*, 61: 114-123. doi:10.1016/j.atmosenv.2012.07.028